



LUND UNIVERSITY

A comparison of two numerical methods for homogenization of Maxwell's equations

Engström, Christian; Sjöberg, Daniel

2004

[Link to publication](#)

Citation for published version (APA):

Engström, C., & Sjöberg, D. (2004). *A comparison of two numerical methods for homogenization of Maxwell's equations*. (Technical Report LUTEDX/(TEAT-7121)/1-10/(2004); Vol. TEAT-7121). [Publisher information missing].

Total number of authors:

2

General rights

Unless other specific re-use rights are stated the following general rights apply:

Copyright and moral rights for the publications made accessible in the public portal are retained by the authors and/or other copyright owners and it is a condition of accessing publications that users recognise and abide by the legal requirements associated with these rights.

- Users may download and print one copy of any publication from the public portal for the purpose of private study or research.
- You may not further distribute the material or use it for any profit-making activity or commercial gain
- You may freely distribute the URL identifying the publication in the public portal

Read more about Creative commons licenses: <https://creativecommons.org/licenses/>

Take down policy

If you believe that this document breaches copyright please contact us providing details, and we will remove access to the work immediately and investigate your claim.

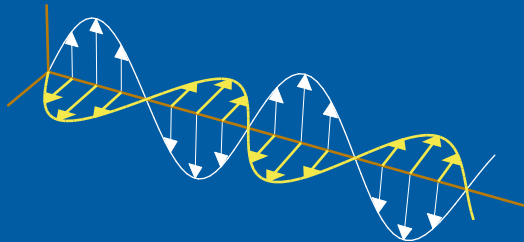
LUND UNIVERSITY

PO Box 117
221 00 Lund
+46 46-222 00 00

A Comparison of Two Numerical Methods for Homogenization of Maxwell's equations

Christian Engström and Daniel Sjöberg

Department of Electrosience
Electromagnetic Theory
Lund Institute of Technology
Sweden



Christian Engström and Daniel Sjöberg

Department of Electrosience

Electromagnetic Theory

Lund Institute of Technology

P.O. Box 118

SE-221 00 Lund

Sweden

Editor: Gerhard Kristensson

© Christian Engström and Daniel Sjöberg, Lund, February 5, 2004

Abstract

When the wavelength is much larger than the typical scale of the microstructure in a material, it is possible to define effective or homogenized material coefficients. The classical way of determination of the homogenized coefficients consists of solving an elliptic problem in a unit cell. This method and the Floquet-Bloch method, where an eigenvalue problem is solved, are numerically compared with respect to accuracy and contrast sensitivity. The Floquet-Bloch method is shown to be a good alternative to the classical homogenization method, when the contrast is modest.

1 Introduction

In the study of composite materials one is concerned with the study of a material with microstructure. When the period of the structure is small compared to the wavelength, the coefficients in Maxwell's equations oscillate rapidly. The oscillating coefficients give rise to numerical problems, which are hard to overcome when the period is very small compared to the wavelength. To handle the numerical problem various kinds of methods have been developed. A multiscale finite element method, particularly suitable for problems with many scales, has been developed for scalar elliptic problems, see [10]. In [1] the authors applied a finite difference method for the same type of problems. The purpose of homogenization is to replace the rapidly oscillating coefficients with new effective constant coefficients. The coefficients are some times random and some times, as in this paper, periodic. A detailed exposition on the subject can be found in the books [2] and [11]. Among the many papers on the topic, we mention a wavelet-based numerical homogenization method introduced in [8], suitable for non-periodic problems. In [6], the authors compare the classical method of homogenization and Floquet-Bloch homogenization for scalar elliptic equations, in one and two dimensions. We perform calculations in two and three dimensions for Maxwell's equations.

This paper is organized as follows. The problem is formulated in Section 2. In Section 3 basic results from the classical homogenization method are presented. Results from the Floquet-Bloch method can be found in Section 4. The numerical implementation used in this paper is given in Section 5 and the numerical experiments are presented in Section 6.

2 Formulation of the problem

The material is modelled by the relative permittivity matrix ϵ and the relative permeability matrix μ . The time-harmonic Maxwell equations (time convention $e^{-i\omega t}$) in a source-free region are

$$\begin{aligned} \nabla \times \mathbf{E} &= i\omega\mu_0\mu\mathbf{H}, & \nabla \cdot (\epsilon\mathbf{E}) &= 0, \\ \nabla \times \mathbf{H} &= -i\omega\epsilon_0\epsilon\mathbf{E}, & \nabla \cdot (\mu\mathbf{H}) &= 0, \end{aligned} \tag{2.1}$$

where the permittivity and permeability of vacuum are denoted ϵ_0 and μ_0 respectively. The speed of light in vacuum is $c_0 = 1/\sqrt{\epsilon_0\mu_0}$. The first order Maxwell system (2.1) can be written as a second order system in \mathbf{H}

$$\begin{cases} \nabla \times (\boldsymbol{\epsilon}^{-1} \nabla \times \mathbf{H}) = (\omega/c_0)^2 \boldsymbol{\mu} \mathbf{H}, \\ \nabla \cdot (\boldsymbol{\mu} \mathbf{H}) = 0. \end{cases} \quad (2.2)$$

In the two-dimensional TM case, $\mathbf{H} = H_3(x_1, x_2) \hat{\mathbf{x}}_3$, with vacuum permeability $\boldsymbol{\mu} = \mathbf{I}$, the system (2.2) becomes

$$-\nabla \cdot (\boldsymbol{\epsilon}^{-1} \nabla H_3) = (\omega/c_0)^2 H_3. \quad (2.3)$$

The coefficients $\boldsymbol{\epsilon} = \boldsymbol{\epsilon}_\delta(\mathbf{x})$ are assumed to be δ -periodic, where δ is a small number. Matrices of the form $\boldsymbol{\epsilon}_\delta(\mathbf{x}) = \boldsymbol{\epsilon}(\mathbf{x}/\delta)$ are then unit-periodic in $\mathbf{y} = \mathbf{x}/\delta$.

For a fixed δ the solution \mathbf{H} is described by two scales, the macroscopic variable \mathbf{x} and the microscopic variable $\mathbf{y} = \mathbf{x}/\delta$. When the period δ goes to zero, the limit solution, depending on \mathbf{x} alone, satisfies a system of partial differential equations with constant coefficients (which is a model of a homogeneous material). These constants are the homogenized, or effective, material parameters obtained from problems in the microscopic variable \mathbf{y} over one unit cell. Since the solution does not oscillate rapidly over one cell, this avoids the numerical problems associated with solving the full problem.

3 Classical homogenization

Assume that the permittivity matrix $\boldsymbol{\epsilon}$ is symmetric, and its eigenvalues are bounded between positive constants, not depending on position. Let $\langle f \rangle$ denote the average over the unit cell $U = [0, 1]^n$ in n dimensions and \mathbf{u}_0 an arbitrary constant vector. Denote by $H_{\text{per}}^1(U)$ the space of U -periodic functions belonging to $H^1(U)$, the space of functions f that together with $\partial f/\partial x_i$ are square integrable over U ¹. The homogenized relative permittivity $\boldsymbol{\epsilon}^h$ is defined as, see [2, 5] for a derivation,

$$\boldsymbol{\epsilon}^h \mathbf{u}_0 = \langle \boldsymbol{\epsilon}(\mathbf{u}_0 - \nabla \chi) \rangle, \quad (3.1)$$

where $\chi \in H_{\text{per}}^1(U)$ is a solution to the local problem

$$\nabla \cdot [\boldsymbol{\epsilon}(\mathbf{u}_0 - \nabla \chi(\mathbf{y}))] = 0, \quad \mathbf{y} \in U, \quad n = 2, 3. \quad (3.2)$$

The solution of this electrostatic problem is unique if we impose the condition $\langle \chi \rangle = 0$. A physical motivation to equation (3.2) is that $\nabla \chi$ represent the microscopic part of the field, and \mathbf{u}_0 represents the macroscopic part. Due to the duality relation, [2, p. 663], we can equivalently calculate

$$\begin{cases} \nabla \times [\boldsymbol{\epsilon}^{-1}(\mathbf{u}_0 - \nabla \times \boldsymbol{\psi}(\mathbf{y}))] = 0, & \mathbf{y} \in U \quad n = 3 \\ \nabla \cdot \boldsymbol{\psi} = 0 \end{cases} \quad (3.3)$$

¹More precisely $H_{\text{per}}^1(U)$ is the closure of $C_{\text{per}}^\infty(U)$ in the norm $\|f\| = \sqrt{\|f\|_{L^2(U)}^2 + \sum_{i=1}^n \|\frac{\partial f}{\partial x_i}\|_{L^2(U)}^2}$

and define the homogenized inverse permittivity as

$$(\epsilon^{-1})^h \mathbf{u}_0 = \langle \epsilon^{-1}(\mathbf{u}_0 - \nabla \times \boldsymbol{\psi}) \rangle. \quad (3.4)$$

In the two-dimensional TM case we have

$$\nabla \cdot [\epsilon^{-1}(\mathbf{u}_0 - \nabla \psi(\mathbf{y}))] = 0, \quad \mathbf{y} \in U, \quad n = 2 \quad (3.5)$$

and

$$(\epsilon^{-1})^h \mathbf{u}_0 = \langle \epsilon^{-1}(\mathbf{u}_0 - \nabla \chi) \rangle. \quad (3.6)$$

4 Floquet-Bloch homogenization

When a wave propagates in a homogeneous medium, we use plane waves $e^{i\mathbf{k}\cdot\mathbf{y}}$ to solve the problem. If the medium is heterogeneous and periodic it is natural to look for solutions that can be written on the form

$$\mathbf{H} = \mathbf{v}(\mathbf{y})e^{i\mathbf{k}\cdot\mathbf{y}}, \quad \mathbf{k} \in U' = [-\pi, \pi]^n, \quad (4.1)$$

where $\mathbf{v}(\mathbf{x} + \mathbf{m}) = \mathbf{v}(\mathbf{y})$, $\mathbf{m} \in \mathbb{Z}^n$. The vector \mathbf{k} is the Floquet-Bloch wave vector representing the mismatch of the wavelength with the lattice. The Floquet-Bloch waves, for Maxwell's equations, are solutions of (2.2) that have the form (4.1). Since $\nabla \times (\mathbf{v}(\mathbf{y})e^{i\mathbf{k}\cdot\mathbf{y}}) = e^{i\mathbf{k}\cdot\mathbf{y}}(\nabla + i\mathbf{k}) \times \mathbf{v}(\mathbf{y})$, the eigenvalue problem can be written

$$\begin{cases} (\nabla + i\mathbf{k}) \times [\epsilon^{-1}(\nabla + i\mathbf{k}) \times \mathbf{v}_n] = \frac{\omega_n^2}{c_0^2} \mathbf{v}_n, \\ (\nabla + i\mathbf{k}) \cdot \mathbf{v}_n = 0, \quad \mathbf{y} \in U, \quad n = 3, \end{cases} \quad (4.2)$$

with periodic boundary conditions. In the two-dimensional TM case we have the eigenvalue problem

$$-(\nabla + i\mathbf{k}) \cdot [\epsilon^{-1}(\nabla + i\mathbf{k})\mathbf{v}_n] = \frac{\omega_n^2}{c_0^2} \mathbf{v}_n, \quad \mathbf{y} \in U, n = 2. \quad (4.3)$$

The Floquet-Bloch waves were introduced by Floquet [9] and Bloch [4]. Properties of the Floquet-Bloch waves can be found in [14] and [16]. The homogenized relative permittivity is given by the Hessian of the lowest eigenvalue ω_0^2 at $\mathbf{k} = 0$

$$(\epsilon^{-1})_{ij}^h = \frac{1}{2c_0^2} \frac{\partial^2 \omega_0^2}{\partial k_i \partial k_j}(0), \quad (4.4)$$

see [2] or [7] for a derivation. We give a simple physical motivation. Using $\omega_0(0) = 0$ we obtain

$$\frac{1}{2c_0^2} \frac{\partial^2 \omega_0^2}{\partial k^2}(0) = \frac{1}{c_0^2} \left(\frac{\partial \omega_0}{\partial k}(0) \right)^2, \quad (4.5)$$

where $\frac{\partial \omega_0}{\partial k}(0)$ is the group velocity. In an isotropic non-magnetic homogeneous medium we have $\frac{\partial \omega_0}{\partial k}(0) = \omega/k$ and $\omega/k = c_0/\sqrt{\epsilon}$. Then follows

$$\frac{1}{2c_0^2} \frac{\partial^2 \omega_0^2}{\partial k^2}(0) = \epsilon^{-1}, \quad (4.6)$$

which justifies (4.4). In the case of electron dynamics in metals, (4.4) corresponds to the effective mass, see for instance [13, p. 193].

5 Numerical implementation

5.1 Classical method

Suppose that the permittivity matrix is isotropic, $\epsilon = \epsilon \mathbf{I}$. The diagonal elements of the homogenized matrix, ϵ_{ii}^h , are then, in the two-dimensional TM case, given by the minimization problems

$$\epsilon_{ii}^h = \min_{\chi \in H_{\text{per}}^1(U)} \int \epsilon |\nabla \chi + \hat{\mathbf{e}}_i|^2 dy \quad (5.1)$$

or

$$(\epsilon^{-1})_{ii}^h = \min_{\chi \in H_{\text{per}}^1(U)} \int \epsilon^{-1} |\nabla \chi + \hat{\mathbf{e}}_i|^2 dy. \quad (5.2)$$

The solutions of these problems are equivalent with the solutions of the differential equations (3.2) and (3.5), see [11, p. 39]. Let V be any finite-element subspace of $H_{\text{per}}^1(U)$. Denote by ϵ_{ii}^+ , ϵ_{ii}^- the solution of (5.1), (5.2) where the minimum is taken over V . Since the minimum is then taken over a smaller space, it follows that $\epsilon_{ii}^h \leq \epsilon_{ii}^+$ and $(\epsilon_{ii}^h)^{-1} \leq (\epsilon_{ii}^-)^{-1}$. That means

$$\epsilon_{ii}^- \leq \epsilon_{ii}^h \leq \epsilon_{ii}^+. \quad (5.3)$$

We use these numerical estimates in the two-dimensional TM case and $\epsilon_{ii}^h \leq \epsilon_{ii}^+$ in the three-dimensional case. All calculations are performed with the MATLAB toolbox FEMLAB, which uses a standard Galerkin implementation.

5.2 Floquet-Bloch method

The eigenvalues $\omega^2(\mathbf{k})$ are symmetric with respect to the origin and $\omega^2(0) = 0$. This gives us a second order, $o(h^2)$, finite difference formula for the second partial derivatives

$$\begin{aligned} \frac{\partial^2 \omega^2(0)}{\partial k_1^2} &= \frac{1}{h^2} \omega^2(h\hat{\mathbf{e}}_1), \\ \frac{\partial^2 \omega^2(0)}{\partial k_1 \partial k_2} &= \frac{1}{2h^2} [\omega^2(h\hat{\mathbf{e}}_1 + h\hat{\mathbf{e}}_2) - \omega^2(h\hat{\mathbf{e}}_1 - h\hat{\mathbf{e}}_2)]. \end{aligned} \quad (5.4)$$

These formulas are used in most calculations. The error in the calculations in Section 6 are not in the approximation of the derivatives. When the number of nodes is small, the discretization error dominates. In one case, Figure 3, a fourth-order finite difference formula is used

$$\frac{\partial^2 \omega^2(0)}{\partial k_1^2} = \frac{1}{6h^2} [16\omega^2(h\hat{\mathbf{e}}_1) - \omega^2(2h\hat{\mathbf{e}}_1)]. \quad (5.5)$$

In the two-dimensional case the calculations are done with the MATLAB toolbox FEMLAB, which uses a Krylov subspace method (Arnoldi's method), see [15]. The calculations for the three-dimensional inclusions are performed with the freely available MIT Photonic-Bands package, described in [12]. The MIT program uses the fast Fourier transform (FFT), which gives a very fast algorithm compared to FEMLAB.

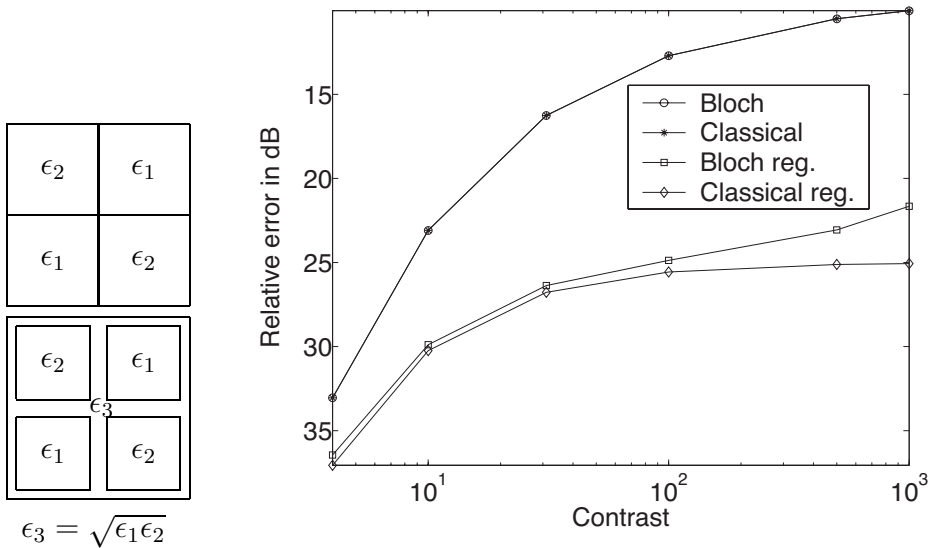


Figure 1: Relative error as a function of contrast (log scale). The Floquet-Bloch vector is $\mathbf{k} = (0.01, 0)$ and the number of nodes are about 6200. Both methods are sensitive to contrast in the standard checkerboard case (upper geometry). The Floque-Bloch (Bloch) and classical solutions are approximately equal. The classical solution (Classical reg.) of the regularization of the checkerboard problem (lower geometry) is less sensitive to contrast than the Floquet-Bloch solution (Bloch reg.). In this case the side length of the squares are 0.4.

6 Numerical results

6.1 The two-dimensional TM case

Explicit formulas for the homogenized matrix can in general only be found in the one-dimensional case. In two dimensions it is possible to calculate an explicit formula if the matrix ϵ satisfies the symmetry condition

$$\epsilon(\mathbf{y})\epsilon(\mathbf{R}\mathbf{y}) = c\mathbf{I} \quad (6.1)$$

where c is a positive constant and

$$\mathbf{R} = \begin{pmatrix} 0 & 1 \\ -1 & 0 \end{pmatrix} \quad (6.2)$$

is the matrix associated with the rotation by the angle $\pi/2$. It can be shown that

$$\epsilon^h = \sqrt{c}\mathbf{I}. \quad (6.3)$$

see, [11, pp. 35-36]. We consider problems with checkerboard structure as in Figure 1 and Figure 2, which all have the analytic solution $\epsilon^h = \sqrt{\epsilon_1\epsilon_2}\mathbf{I}$. The analytic result is compared with numerical computations of the classical solution (3.1) and the Floquet-Bloch solution (4.4). Due to the behavior of the field near corner

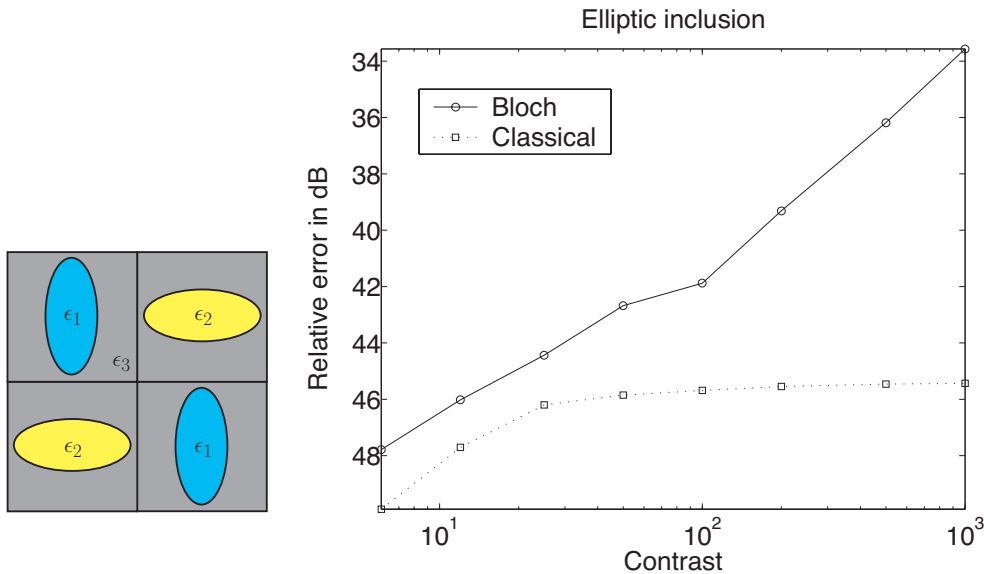


Figure 2: Relative error as a function of contrast (log scale), when $\epsilon_3 = \sqrt{\epsilon_1\epsilon_2}$ and the semi axes are (0.24, 0.20). The number of nodes are 2080 and the Floquet-Bloch vector is $\mathbf{k} = (0.01, 0)$. The classical solution is not sensitive to contrast.

points, the standard checkerboard in Figure 1 is numerically difficult, see [3]. We cannot expect small errors with standard FEM. From a physical point of view the question is whether the inclusions are touching or not. The classical method and the Floquet-Bloch method are equally bad in this case.

A possible regularization of the standard checkerboard problem is to put in a new material ϵ_3 between the squares, see Figure 1. The error with $\epsilon_3 = \sqrt{\epsilon_1\epsilon_2}$ is considerably lower and the error in the classical method is not so sensitive to contrast.

The relative error as a function of contrast, for elliptical inclusions, is shown in Figure 2. The classical solution is astonishingly good at high contrasts, but even in the worst case the Floquet-Bloch method gives us three correct digits.

In the case of a simple square inclusion, as in Figure 3, we do not have an analytical solution, but we have the numerical bounds (5.3). Using the approximation $\epsilon^h = (\epsilon^+ + \epsilon^-)/2$ with the maximum error $(\epsilon^+ - \epsilon^-)/2$, we get $\epsilon^h = 1.54422 \pm 2 \cdot 10^{-5}$ with the classical method. In the figure, the Classical High/Low corresponds to ϵ^+/ϵ^- . The convergence of the Floquet-Bloch solution depends on the chosen k . If $k = 0.001$ is chosen and the derivatives are approximated with a second order finite difference formula, then the algorithm seems to be unstable. The smallest eigenvalue is 10^4 times smaller when $k = 0.001$ is used. This probably cause a larger relative error. The solution is much better if we choose $k = 0.1$ and use a fourth order finite difference formula. The accuracy can be improved even further by using Richardson extrapolations.

When the fourth order approximation (5.5) is used, we need two points instead of only one. The computation time for the solution of the classical problem is

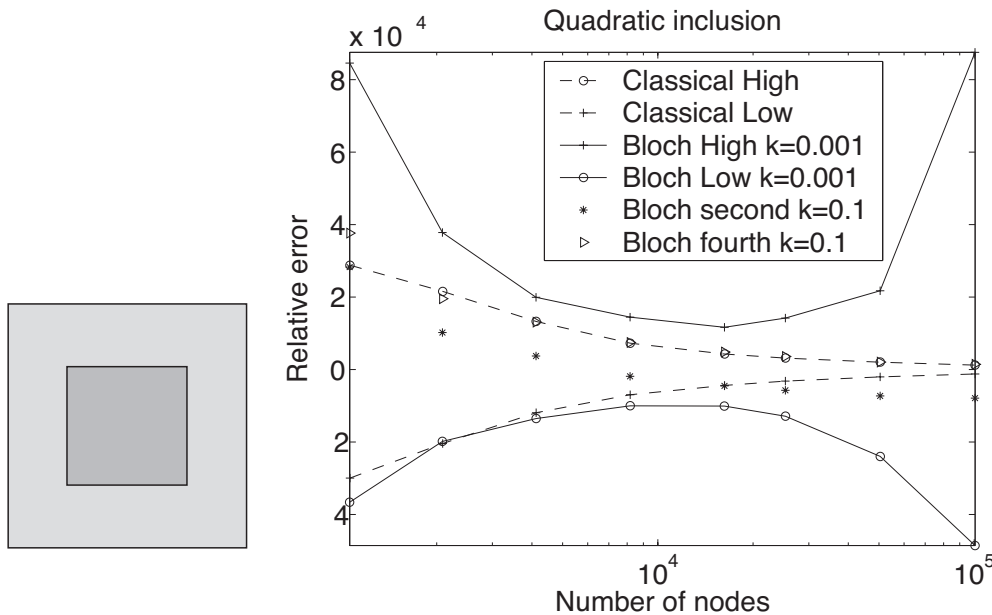


Figure 3: Relative error as a function of the number of nodes (log scale), when the contrast is ten and the side length of the square is 0.5. The error is the normalized distance, with sign, to $\epsilon^h = 1.54422$, which is the arithmetic mean of Classical High and Classical Low, when the number of nodes are 10^5 . Bloch High is the usual Floquet-Bloch solution, calculated with ϵ and Bloch Low is calculated with ϵ^{-1} . All Floquet-Bloch solutions except '▷' are calculated with the second order finite difference formula (5.4). In the Floquet-Bloch solution '▷', the fourth order formula (5.5) is used. This solution is very close to the classical solution.

almost equal to the time for the solution of the Floquet-Bloch problem when the second order approximation is used. If the fourth order approximation is used, the computation time is twice the time for the classical problem. In the anisotropic case we need two and eight points for the second and fourth order approximation, respectively.

6.2 Three dimensions

In the case of spherical inclusions Figure 4, we do not have an explicit formula, but we know that the solution should approach the Maxwell-Garnett formula (lower bound in Figure 4) when the radius goes to zero. Figure 4 shows that we have good agreement with the Maxwell-Garnett formula and between the different methods. The classical solution provides an upper bound. The Floquet-Bloch solution is slightly above the bound, but this probably depends on the different grid, that is used by the MIT program. The MIT program uses a uniform grid and FEMLAB uses a grid that adapts to the geometry.

To get a problem with an analytical solution we extend a two-dimensional checkerboard problem to three dimensions, see Figure 5. The error is considerably

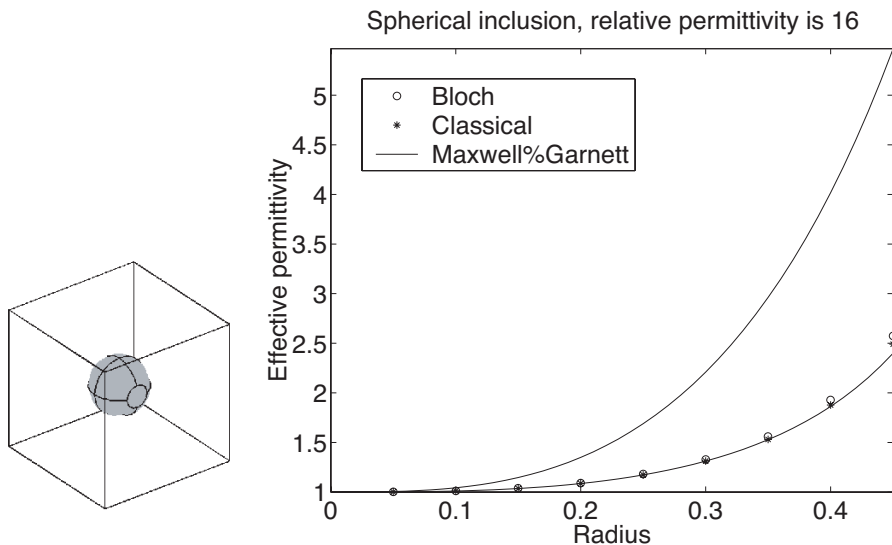


Figure 4: Relative permittivity is 16. The number of elements in the classical solution is 107716 and in the Floquet-Bloch solution 262144 elements are used. The Floquet-Bloch vector is $\mathbf{k} = (0.1, 0, 0)$. The lower Maxwell-Garnett bound is $\epsilon_b + 3f\epsilon_b(\epsilon_i - \epsilon_b)/(\epsilon_i + 2\epsilon_b - f(\epsilon_i - \epsilon_b))$, where f is the volume fraction of the inclusion and ϵ_i , ϵ_b is the permittivity of the inclusion and the background material, respectively. If the inclusion and the background material are exchanged, the upper bound is described by the same formula. The Maxwell-Garnett formula is a very good approximation when the radius is small.

larger if we calculate the problem in three dimensions, compare Figure 2 and Figure 5. The FFT based MIT program uses the effective-medium technique, see [12], to handle the discontinuity of ϵ . The algorithm works well for modest contrasts, but cannot handle large contrasts.

7 Discussion and conclusions

In the two-dimensional cases a finite-element algorithm is used in both methods. The classical method works better when the contrast is high, but the Floquet-Bloch solution can probably be improved if a good preconditioner is used. For instance a generic incomplete LU factorization algorithm with threshold is used in [15, p. 288] to solve a similar problem.

In the three-dimensional cases a finite-element algorithm, FEMLAB, is used for the classical method and a FFT based algorithm, from MIT, for the Floquet-Bloch method. The MIT program is considerably faster than FEMLAB, but it does not work well for high contrasts. As in the two-dimensional cases, a finite-element algorithm with a good preconditioner, will probably give better accuracy when the contrast is high. The Floquet-Bloch method is shown to be a good alternative to the classical homogenization method, when the contrast is modest.

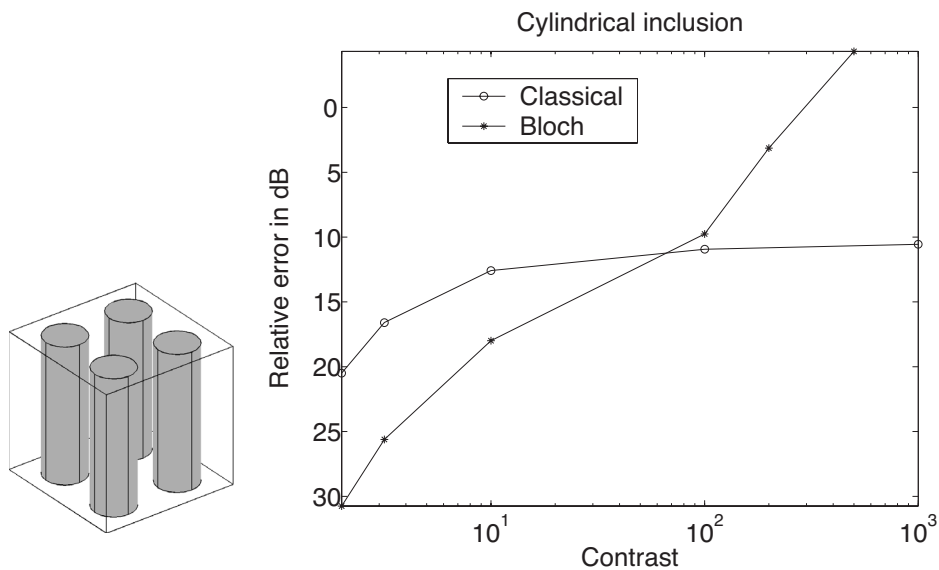


Figure 5: Relative error as a function of contrast, when the radius of the cylinders is 0.2. The number of elements in the classical solution are 398453 and in the Floquet-Bloch solution 262144 elements are used. The Floquet-Bloch vector is $\mathbf{k} = (0.1, 0, 0)$. The Floquet-Bloch solution is accurate for modest contrasts, but bad for high contrasts.

References

- [1] M. Avellaneda, T. Hou, and G. Papanicolaou. Finite difference approximations for partial differential equations with rapidly oscillating coefficients. *Math. Modell. Numer. Anal.*, **25**(6), 693–710, 1991.
- [2] A. Bensoussan, J. L. Lions, and G. Papanicolaou. *Asymptotic Analysis for Periodic Structures*, volume 5 of *Studies in Mathematics and its Applications*. North-Holland, Amsterdam, 1978.
- [3] S. Berggren, D. Lukkassen, and A. Meidell. A new method for numerical solution of checkerboard fields. *Journal of Applied Mathematics*, **1**(4), 157–173, 2001.
- [4] F. Bloch. Über die Quantenmechanik der Electronen in Kristallgittern. *Z. Phys.*, **52**, 555–600, 1928.
- [5] D. Cioranescu and P. Donato. *An Introduction to Homogenization*. Oxford University Press, Oxford, 1999.
- [6] C. Conca and S. Natesan. Numerical methods for elliptic partial differential equations with rapidly oscillating coefficients. *Comput. Methods Appl. Mech. Engrg.*, **192**, 47–76, 2003.

- [7] C. Conca and M. Vanninathan. Homogenization of periodic structures via Bloch decomposition. *SIAM J. Appl. Math.*, **57**(6), 1639–1659, 1997.
- [8] M. Dorobantu and B. Engquist. Wavelet-based numerical homogenization. *SIAM Journal on Numerical Analysis*, **35**(2), 540–559, 1998.
- [9] G. Floquet. Sur les équations différentielles linéaires à coefficients périodique. *Ann. École Norm. Sup.*, **12**, 47–88, 1883.
- [10] T. Y. Hou, X. H. Wu, and Z. Cai. Convergence of a multiscale finite element method for elliptic problems with rapidly oscillating coefficients. *Mathematics of Computation*, **68**(227), 913–943, 1999.
- [11] V. V. Jikov, S. M. Kozlov, and O. A. Oleinik. *Homogenization of Differential Operators and Integral Functionals*. Springer-Verlag, Berlin, 1994.
- [12] S. G. Johnson and J. D. Joannopoulos. Block-iterative frequency-domain methods for Maxwell’s equations in a planewave basis. *Opt. Express*, **8**(3), 173–190, 2001.
- [13] C. Kittel. *Introduction to Solid State Physics*. John Wiley & Sons, New York, 6 edition, 1986.
- [14] F. Odeh and J. B. Keller. Partial differential equations with periodic coefficients and Bloch waves. *J. Math. Phys.*, **5**, 1499–1504, 1964.
- [15] Y. Saad. *Iterative Methods for Sparse Linear Systems*. PWS Publishing Company, Boston, 1996.
- [16] C. H. Wilcox. Theory of Bloch waves. *Journal d’analyse mathématique*, **33**, 146–167, 1978.